Title

Spatially organizing biochemistry: choosing a strategy to translate synthetic biology to the factory

Authors and Affiliations

Christopher M. Jakobson[1], Danielle Tullman-Ercek[2], Niall M. Mangan[3]*

[1]Department of Chemical and Systems Biology, Stanford University School of Medicine, Stanford CA 94305

[2]Department of Chemical and Biological Engineering, Northwestern University, Evanston IL 60208

[3]Department of Engineering Science and Applied Mathematics, Northwestern University, Evanston IL 60208

*To whom correspondence should be addressed: niallmm@gmail.com

Abstract

Natural biochemical systems are ubiquitously organized both in space and time. Engineering the spatial organization of biochemistry has emerged as a key theme of synthetic biology, with numerous technologies promising improved biosynthetic pathway performance. One strategy, however, may produce disparate results for different biosynthetic pathways. We propose a spatially resolved kinetic model to explore this fundamental design choice in systems and synthetic biology. We predict that two example biosynthetic pathways have distinct optimal organization strategies that vary based on pathway-dependent and cell-extrinsic factors. Moreover, we outline this design space in general as a function of kinetic and biophysical properties, as well as culture conditions. Our results suggest that organizing biosynthesis has the potential to substantially improve performance, but that choosing the appropriate strategy is key. The flexible mathematical framework we propose can be adapted to diverse biosynthetic pathways, and lays a foundation to rationally choose organization strategies for biosynthesis.

Introduction

Synthetic biology traces its origins to the discovery of type II restriction endonucleases (Kelly and Smith, 1970; Smith and Welcox, 1970). These enzymes allowed the controlled assembly of novel genes, plasmids, and other nucleic acids, and precipitated the rapid spread of molecular cloning technology. Since then, synthetic biology has sought to exploit, adapt, and extend biological systems to benefit society by creating pharmaceuticals, fuels, gene therapies, drug delivery platforms, probiotics, and more. Metabolic engineering, the use of microbes to produce small and large molecules of commercial and scientific interest, has been a particular focus. To this end, synthetic biologists have developed methods to control transcription and translation, knock out native genes to route metabolic flux down desired channels, integrate multiple chemical and physical inputs to make decisions inside microbial cells, and make wholesale changes to the genomes of organisms in high throughput.

A new paradigm in synthetic biology technologies focuses on a new challenge: spatiotemporal organizational of biochemical processes. Organisms in all domains of life exert fine control over when and where biochemical reactions occur, be they responsible for metabolism, information transfer, or cell replication. This kind of organization remains conspicuously absent from most engineered systems.

Early efforts in synthetic biology focused on the creation of generalized systems to transcribe and translate heterologous genes and proteins in a variety of hosts, from bacteria to fungi to mammalian cells. These included the creation of modular libraries of

genetic parts, such as plasmids, promoters, terminators, and ribosome binding sites (Beal et al., 2014; Blazeck et al., 2012b, 2012a; Brophy and Voigt, 2016; Dahl et al., 2013; Fernandez-Rodriguez and Voigt, 2016; Leavitt et al., 2016; Lee et al., 2013, 2015; Mutalik et al., 2013; Rajkumar et al., 2016; Salis et al., 2009). It is now possible to computationally design composable genetic circuits based on these parts with high fidelity (Nielsen et al., 2016; Roehner et al., 2016). Efforts were also made to understand and control translation elongation, and inform the choice of codons in heterologous genes (Goodman et al., 2013).

Along with the introduction of foreign genes into microbial factories, it was soon recognized that removing host genes was also of critical importance. Sophisticated computational approaches now exist to predict which native genes should be removed from a microbe in order to maximize the yield of a desired biosynthetic product (Burgard et al., 2003; Price et al., 2004; Alper et al., 2005; Kim et al., 2008). These models can also include predictions of host or foreign genes whose introduction might be beneficial (Ranganathan et al., 2010; Srivastava et al., 2012).

Cellular computation, enabling cells to collect information from their environment and make decisions accordingly, has also been an important focus of synthetic biology (Purcell and Lu, 2014), but will not be discussed further here. Instead we will focus on metabolic engineering applications.

Despite all of these technological advances, there have been relatively few examples of the commercially successful, industrial scale production of chemicals by microbes (Lechner et al., 2016). Notable successes have included artemisinic acid (Paddon et al., 2013), as well as farnesene, 1,3-propanediol, and 1,4-butanediol (Lechner et al., 2016), but, by and large, the biological production of chemicals at industrially viable titers has remained elusive. This is most often due to one (or more) of five ubiquitous roadblocks to biosynthesis: cellular toxicity due to accumulation of intermediates of the biosynthetic pathway; the loss of flux to undesired byproducts; difficulties sustaining sufficient substrate influx; leakage and loss of intermediates into the culture medium; and trapping of product in the host cell due to inadequate efflux [Fig. 1A].

A new wave of synthetic biology technologies aims to address these key issues using a diverse array of strategies, while also preparing to deploy engineered microbes widely and safely. These cutting-edge approaches include cell-free approaches to protein and small molecule synthesis (Dudley et al., 2016; Garamella et al., 2016; Goering et al., 2016; Lu et al., 2015, 2014; Sullivan et al., 2016; Worst et al., 2015), dynamic control of metabolite concentrations (Xu et al., 2014) and of transcription and translation at the RNA level (Chappell et al., 2015; Takahashi and Lucks, 2013), robust approaches to biocontainment (Lopez and Anderson, 2015; Mandell et al., 2015), sensing of diverse small molecules (Mukherjee et al., 2015), establishing consortia of synergistic microbes (Marchand and Collins, 2016; Peng et al., 2016), and discovering enzymes facilitating previously unknown catalyses (Walker et al., 2013; Zhu et al., 2015). Broadly speaking, these strategies address a key missing capability in the synthetic biological toolkit: the

ability to control precisely when and where chemical reactions take place (Boyle and Silver, 2012; Kerfeld, 2017; Kim and Tullman-Ercek, 2013).

Here, we will analyze one class of these strategies: the spatial organization of metabolism within cells [Fig. 1B] (Polka et al., 2016). There are a wide variety of natural methods for spatial organization (Agapakis et al., 2012). Eukarya discretize their biochemistry into highly chemically distinct subcellular compartments and into enzyme complexes such as polyketide synthases (Khosla et al., 2014) and other metabolons (Wu and Minteer, 2014). Bacteria, too, are now understood to organize their metabolism in a variety of ways, including using protein-based carboxysomes (Shively et al., 1973), microcompartments (Bobik et al., 1999), and encapsulins (McHugh et al., 2014). 1,2-propanediol utilization (Pdu) microcompartments, for instance, are protein-bound organelles of approximately 150 nm diameter. The enclosing protein shell consists of trimeric, pentameric, and hexameric protein tiles with central pores that permit the passage of small molecules in and out of the organelles, but which prohibit the passage of enzymes and other proteins. Building on foundational microbiological understanding of these systems (Bobik et al., 1999; Fan et al., 2010; Huseby and Roth, 2013; Kerfeld et al., 2005; Kofoid et al., 1999), we and others have demonstrated control of the formation (Kim et al., 2014), protein content (Jakobson et al., 2015; Lawrence et al., 2014; Parsons et al., 2010; Wagner et al., 2016), catalytic activity (Jakobson et al., 2016), and transport properties (Slininger Lee et al., 2017) of these organelles. Due to their relative simplicity and ease of manipulation, these various protein-based compartments make excellent model systems for exploring the role of spatial organization on metabolism.

Likewise, much work has been done to characterize carboxysomes—compartments in which CO_2 is concentrated to enhance carboxylation in photosynthetic bacteria-- and adapt them for engineering purposes (Cai et al., 2015, 2016; Chen et al., 2013). The modularity of carboxysomes and other CO_2 concentrating mechanism components facilitates reconstitution in other organisms (Bonacci et al., 2012; Gonzalez-Esquer et al., 2015). An active area of research is reconstitution in plants (Lin et al., 2014a, 2014b; Long et al., 2015), as part of a broad strategy to increase plant yields (Giessen and Silver, 2017; Hanson et al., 2016; Rae et al., 2017; Sharwood et al., 2016). Engineering microbial metabolism with CO_2 as the primary carbon source would allow the production of sustainably produced biofuels and other high value products (Antonovsky et al., 2016; Ducat and Silver, 2012) and carboxysomes could enhance such strategies. More generally, ccarboxysomes have been suggested as modular method for partitioning non-native pathways from native metabolism (Kerfeld, 2017). However, we have strong indication that performance of CO_2 concentrating mechanisms will depend on how encapsulation interplays with transporters or other exogenous conditions setting the supply of CO_2 (Mangan and Brenner, 2014; Mangan et al., 2016), and further systems analysis is required to realize the benefits of carboxysome-based encapsulation (Hanson et al., 2016; Long et al., 2016).

Bacterial microcompartment organelles are not the only organization solution available to the metabolic engineer; scaffolds based on protein, lipid, DNA, and RNA have all shown promise in improving heterologous pathway performance. Each of these strategies have

146 been shown to be effective for the enhancement of heterologous biosynthesis in various
147 contexts (Conrado et al., 2012; Delebecque et al., 2011; Dueber et al., 2009; Lawrence et
148 al., 2014; Moon et al., 2010; Myhrvold et al., 2016). These studies organized diverse
149 biosyntheses, including of mevalonate, resveratrol, 1,2-propanediol, and molecular
150 hydrogen, suggesting that many different enzymatic pathways could be enhanced by
151 scaffolding.
152
153 Having developed tools to control the localization of heterologous biosynthetic pathways
154 to these organizing structures, a crucial question remains: what pathways are suitable for
155 organization? And what benefits might be accrued by organizing pathways in one way
156 versus another?
157
158 **Results**
159 *Pathway encapsulation in bacterial microcompartments can provide benefits comparable*
160 *to protein engineering*
161 We will outline the potential metabolic engineering benefits that could be derived from
162 pathway organization using two different strategies: encapsulation in the Pdu
163 microcompartment of *Salmonella* and other enteric bacteria, and organization using a
164 scaffold (which could be organized by means of protein, lipid, or nucleic acid) [Fig. 1C].
165
166 To address the kinetic consequences of encapsulation in these structures, we make use of
167 a computational framework (Jakobson et al., 2017) developed to analyze the native
168 function of the microcompartment organelles. A key prediction of this model is that

169 microcompartments significantly enhance pathway flux. We predict that the natively
170 encapsulated system enjoys a four-order of magnitude enhancement in flux upon
171 encapsulation, as compared to free diffusion of the enzymes in the cytosol (Jakobson et
172 al., 2017). Appropriately chosen heterologous pathways might also accrue such flux
173 enhancements, as well as potentially reducing the loss of pathway intermediates to the
174 extracellular space.
175
176 To instead model a scaffolded system, we simply assume that the enzymes in question
177 are localized to a volume equivalent to that occupied by the Pdu microcompartments, but
178 without a diffusion barrier. This is represented mathematically by setting the velocity of
179 transport between the scaffold volume and the cytosol equal to that predicted by free
180 diffusion. The model formulation we use here is agnostic to the underlying scaffolding
181 platform (protein, lipid, or nucleic acid) or its microscopic organization, as we assume a
182 well-mixed scaffold volume.
183
184 We predict the consequences of organization using these two strategies for two model
185 biochemical processes: native Pdu microcompartment metabolism and the heterologous
186 mevalonate biosynthetic pathway. The compounds and enzyme kinetic parameters for
187 each pathway are in Figure 2AB. We adapt the modeling approach used for the native
188 Pdu system to make flux predictions for the heterologous mevalonate pathway by
189 adjusting the enzymatic kinetic parameters, cell membrane permeability to metabolites,
190 and enzyme abundance and stoichiometry. While the first substrate of the mevalonate
191 pathway (acetoacetyl-CoA) is produced intracellularly, rather than entering from the

192 extracellular space (in the case of 1,2-PD), we approximate the generation of acetoacetyl-
193 CoA upstream as a constant extracellular concentration in the context of our kinetic
194 model. This approximation could correspond to production of acetoacetyl-CoA by a
195 relatively faster and reversible upstream enzyme, or to more complex homeostatic control
196 of the acetoacetyl-CoA concentration in the cytosol, both resulting in an effectively
197 constant concentration of acetoacetyl-CoA far from the organelle or scaffold. Supporting
198 this assumption, we find that the concentration gradient in the cytosol is small across a
199 wide range of external substrate concentrations for all the organizational cases we tested
200 (Fig. S1).
201
202 We first ask: is organization worth the time and trouble for the metabolic engineer to
203 arrange, as compared to traditional metabolic and enzyme engineering strategies (such as
204 improvements to the k_{cat} or K_M kinetic parameters)? Here, we use the native Pdu
205 microcompartment pathway as an example. If, for instance, engineering efforts increased
206 the k_{cat} of each of the two key enzymatic steps 100-fold, or decrease the K_M of each key
207 step 100-fold, the improvement in flux would be as shown in Figure 2CD (as compared
208 to the native system with no organization). Improvements of this magnitude for both
209 enzymes represent a significant technical challenge and would be non-trivial to achieve
210 for an arbitrary enzymatic system. We predict that encapsulation of native Pdu
211 metabolism in an organelle is practically as effective as large improvements in k_{cat}, and
212 more effective than large improvements in K_M, with respect to increasing the total flux
213 through the pathway [Fig. 2C]. See the Methods for a detailed description of this
214 calculation and the model in general. The predicted concentrations of each metabolite for

each kinetic case are shown in Figure S2. The dramatic improvement in predicted flux upon encapsulation is due to a large increase in the intermediate concentration in the vicinity of the second pathway enzyme, exceeding the saturating concentration. Moreover, this benefit comes without a significant increase in the cytosolic concentration of this intermediate [Fig. S2]. Our simulations predict the native Pdu microcompartment metabolic pathway benefits substantially more from encapsulation than it would from scaffolding [Fig. 2C].

On the other hand, the pathway to produce mevalonate accrues similar flux enhancement from an organelle- or scaffold-based organization strategy [Fig. 2D; Fig. S3]. Our prediction agrees with the experimental observation that organizing the mevalonate pathway on a protein scaffold increased titers (Dueber et al., 2009). We predict marginal additional benefit from an encapsulation approach in this case, since the Michaelis-Menten constants K_M for the enzymes are small, whereas we predict the potential for flux enhancement by encapsulation in an organelle is high for pathways kinetically similar to native Pdu metabolism (that is, with larger K_M) [Fig. 2CD; see also Fig. 4B]. These kinds of predictions can be made *a priori* for any enzymatic pathway for which the kinetic parameters are known (or can be approximated).

In both cases, the increased pathway flux in the case of increasing the k_{cat} of each enzymatic step comes at the cost of greatly increased loss of intermediate species to the extracellular space (or to other cellular process, in the case that there are competing reactions in the cytosol) [Figure S4]. This tradeoff may be important to consider in some

cases, for instance if the intermediate species is toxic, and may render the protein engineering strategy less appealing than organization, despite similar predicted flux enhancement.

Optimal organization strategies for biosynthetic pathways differ based on pathway properties and culture conditions

In addition to intrinsic properties of the pathway in question, the benefits of encapsulation versus scaffolding can depend on extrinsic factors, such as the bulk concentration of substrate. At lower external substrate concentrations, flux for pathways organized with scaffolds improves relative to an organelle for both pathways we considered [Fig. 3A]. This is because the rate of entry of substrate into the organelle becomes problematic at low bulk substrate concentrations, when the driving force for transport into the organelle is reduced. The rate of leakage of intermediate to the extracellular space is also affected; in each case, a scaffold leads to the greatest intermediate leakage, and this disadvantage worsens at low bulk substrate concentration for both pathways [Fig. 3B]. This underscores the importance of considering the pathway in question and the desired outcome (flux enhancement or leakage prevention) when selecting organization strategies. Modeling approaches could be extended in future to account for this duality by creating composite objective functions for the energetic cost of flux enhancement and leakage, or for the cost of the enzymes and organizing structures themselves (Noor et al., 2016), and optimizing across these different factors simultaneously.

We next consider the effects of one cell-intrinsic property (the abundance and kinetics of the second pathway enzyme) and one cell-extrinsic property (external substrate concentration) simultaneously [Fig. 3C]. These phase spaces show the optimal organizational strategy to maximize flux as a function of both variables, with the optimal strategy indicated by the color of the phase space at that parameter value combination. For reference, the dashed line in each panel of Figure 3C indicates the $k_{cat}E_0$ value used to construct the one-dimensional representations with respect to S_{ext} in Figure 3A. While the topology of these landscapes is similar for both systems (and indeed for any irreversible two-enzyme pair governed by Michaelis-Menten kinetics), there are important quantitative differences. Critically, given the $k_{cat}E_0$ value of the second enzyme in the mevalonate synthesis pathway, we predict that organelle-type organization is favored at high S_{ext} but scaffolding is favored at low S_{ext} values [Fig. 3C]. A batch-type reactor, therefore, might transition from organelles to scaffolds being optimal during a production run; laboratory-scale pilot experiments are most often conducted in this mode, potentially convoluting different optimality regimes. This observation holds for $k_{cat}E_0$ values several orders of magnitude smaller or larger than our estimate. The same is not true for the native Pdu MCP system, in which organelles are favored for all S_{ext} values given our assumptions regarding $k_{cat}E_0$ of PduP/Q [Fig. 3C]. This kind of information is key in designing optimally productive biosynthetic processes, and might call for a dynamic organizational transition as culture conditions change (Yang et al., 2017).

Finally, we demonstrate how the optimal organizational strategy changes as a function of two intrinsic pathway properties (rather than one intrinsic and one extrinsic property, as

in Fig. 3C). While there are many parameters that can change between pathways, we focus on two key differences between the Pdu MCP system and mevalonate pathway. The values we estimate for the cell membrane permeability to the intermediate and $k_{cat}E_0$ for the second enzyme differ by approximately two orders of magnitude between the two systems. We therefore predicted the optimal organizational strategy as a function of these two parameters, and indicated the location of each enzyme system in this phase space [Fig. 3D]. We set all model parameters besides cell membrane permeability and $k_{cat}E_0$ to the baseline values for the Pdu MCP system. The phase space does not qualitatively change if we instead set all the other parameters to those representative of the mevalonate biosynthetic pathway [Fig. S5]. We constructed the phase space for two external substrate concentrations S_{ext}, 50 mM and 0.5 mM. Crucially, the change in external concentration shifts the boundary between the regions in which scaffold and organelle strategies are optimal. At the lower S_{ext}, mevalonate biosynthesis favors a scaffold over an organelle, while organelle organization is still favored for the Pdu MCP.

Phase spaces of the kind we explore here can be constructed for any pair of parameters, and provide a means to survey the organizational performance landscape comprehensively across a very wide range of possible parameter values. The parameters to explore could include those susceptible to manipulation via culture conditions, such as S_{ext}; those that can in principle be engineered, such as $k_{cat}E_0$; and those that are intrinsic to the relevant biomolecules, such as the cell membrane permeability to the intermediate species. By constructing these phase spaces for a variety of parameters, the metabolic engineer can gain a quantitative understanding of which parameters are critical in

306 determining the optimal organization strategy for a given pathway, and can weigh the
307 ease of altering a given parameter against the potential rewards in terms of engineering
308 goals like pathway flux.
309
310 *Enzyme stoichiometry and kinetics, as well as design goals, influence optimal*
311 *organization strategy*
312 We can address the question of organization choice more generally by examining the
313 relative performance of three strategies (free cytosolic localization of enzymes; scaffolds;
314 and microcompartments) across a wide range of enzyme kinetic parameters. Considering,
315 for instance, the two-enzyme pathway of native Pdu metabolism, we can predict the
316 optimal strategy as we vary the activity ($k_{cat}E_0$) of each enzyme [Fig. 4A]. This variation
317 can represent either the Pdu enzymes or a different enzymatic pathway. In this example,
318 microcompartment organization is favored with respect to maximizing pathway flux
319 unless the respective $k_{cat}E_0$ parameters for both enzymes are sufficiently large to render
320 the effect of concentrating intermediate species in the microcompartment insignificant, in
321 which case a scaffold is recommended. Conversely, for small $k_{cat}E_0$ of both enzymes, a
322 strategy without spatial organization is indicated to minimize intermediate loss [Fig. 4A].
323 These phase space predictions of organization performance can be made for arbitrary
324 organizational strategies and metabolic pathways, given appropriate kinetic models.
325
326 *The chemical character of the substrate and intermediate also have an impact on*
327 *organization choice*

In addition to the kinetic properties of the pathway enzymes, we can consider the effect of different substrates and intermediates on the choice of appropriate organizational strategies. Once again we compute the recommended organization strategy for the native Pdu metabolic pathway, and vary the values of the relevant model parameters. In this case, several parameters could be affected by the chemical character of the species, including transport across the cell membrane and transport in and out of the microcompartment organelle. If, for instance, transport of the substrate and intermediate across the microcompartment shell is slow, scaffold expression may be favored if the K_M of the second enzyme is sufficiently low [Fig. 4B]. On the other hand, if escape of the intermediate across the cell membrane is slow, scaffolding may be favored regardless of enzyme kinetics [Fig. 4C], since the cell itself can perform the organelle's intermediate-concentrating function in this case. It may be possible to optimize the permeability of the microcompartment shell to the kinetics of the desired pathway and broaden the range of conditions under which an organelle is the optimal pathway (Park et al., 2017; Slininger Lee et al., 2017). All of these factors must be considered when choosing an appropriate organization strategy. This is particularly important when comparing biosynthetic pathways with substrates and intermediates of different sizes, which might reasonably be expected to have disparate transport properties at the cell membrane and microcompartment shell.

Enzyme mechanism can alter the potential benefits of organization strategies

In the above examples, we consider irreversible, Menten-Michaelis kinetics for each enzymatic step of each pathway. This assumption holds for the Pdu microcompartment

case, but not for all systems. For example, in the carboxysome, a carbon-fixation organelle of cyanobacteria, a key enzymatic step catalyzing the interconversion of CO_2/HCO_3^- is reversible, limiting the benefit of organelles to concentrate intermediate species (Mangan and Brenner, 2014). Selective permeability of the carboxysome does not result in increased CO_2 concentration (Mangan et al., 2016). The reversibility of the CO_2/HCO_3^- conversion imposes a fundamental limit on the concentration of CO_2 that can be achieved in the organelle [Fig. S6A]; in the microcompartment, on the other hand, selective permeability combined with enzyme irreversibility allows the development of a very high local intermediate concentration if the intermediate is selectively trapped [Fig. S6B; purple line]. The comparison between the reversible and irreversible kinetic models highlights the need to account for detailed aspects of kinetic mechanism, such as cofactors, inhibition, and other dynamic effects. Recent studies have also indicated that the local chemical environment of nucleic acid-based scaffolds can have beneficial effects on enzyme kinetics (Zhang et al., 2016); detailed kinetic effects of this kind can be incorporated into future models as they are elucidated.

Discussion

A fundamental framework for organizational choice

Above, we outline the potential for the spatial organization of heterologous pathways to greatly enhance their performance. This approach compares well with traditional enzyme engineering approaches. Furthermore, we describe a general framework to guide the choice of appropriate organizational strategies for metabolic engineering. Several key parameters must be accounted for: (I) enzyme kinetics; (II) substrate and intermediate

chemical properties; and (III) external culture conditions. Some of these properties, such as the external substrate concentration and the transport properties of the cell membrane, can influence the supply of substrate to the pathway, while others, such as the presence or absence of competing reactions and the transport properties of the organelle boundary, can influence the loss of metabolic flux to off-target species. We outline the use of a general modeling approach to analyze the performance of different organization strategies, and present example organizational recommendations. Moreover, modeling approaches can suggest key experiments (*e.g.* variations of external substrate concentration) that may reveal important discrepancies in the performance of different organization strategies. The MATLAB code used to generate the graphics in this manuscript is freely available on GitHub (URL TBD), and we encourage members of the metabolic engineering and synthetic biology communities to explore the organizational performance landscapes for their own systems of interest. We also welcome suggestions of other useful kinetic or organizational regimes to include in future versions of the model.

Avenues to improve understanding and prediction of optimal spatial organization

The framework above can provide important insights into the choice of optimal organizational strategies for heterologous pathways, but several important aspects of pathway organization remain unexplored. These include product export, cell size and morphology, competitive reactions, and the detailed organization of the organelles or scaffolds within the host cell. The organization of organelles within cells has been

investigated in the context of a constant cytosolic metabolite concentration (Hinzpeter et al., 2017), and future efforts could combine this and our approaches.

Our model as currently implemented can incorporate extensions to explore some of these areas, but some questions, notably the effect of competitive cellular reactions and reactions upstream of the organized process, will require the integration of our model with larger-scale metabolic models of host processes. Exploring the effect of the detailed subcellular localization of the organizing structures themselves will likewise require modifications to our current mathematical framework.

Practical engineering considerations

Within the framework described here, we evaluate only the pathway flux and intermediate leakage predicted for each potential organization strategy, neglecting the difficulty associated with engineering a particular strategy. It may transpire that, for certain pathways, scaffolding proves challenging to implement due to incompatibilities between the requisite protein tags and the enzymes in question, or that the pores of microcompartment shells are fundamentally of low permeability to the substrates of other pathways. Practical experience with these issues will continue to inform the choice of appropriate strategies, and may eventually allow the integration of such practical as well as theoretical considerations into objective functions. We expect that some key experiments, such as assays to quantitatively determine the permeability of protein shells to small molecules, will greatly enhance the predictability of engineering pathways in microcompartments.

Closing thoughts

Organizing biochemistry in both time and space holds tremendous potential to help deliver on the promise of synthetic biology: the ability to produce medically and industrially important molecules at high yield and high titer with minimal environmental disruption. Spatial organization of the kind we advocate is but one of many important approaches; techniques to use multiple (or no) cells, to detect and transport metabolites, and to exert dynamic control on short time scales are of critical importance, as well. We posit that detailed mechanistic models of each of these approaches will be key in building a fundamental theoretical understanding of the optimal strategies to improve the performance of arbitrary biosyntheses.

Materials and Methods

Contact for resource and reagent sharing

For questions and further information regarding software and models used herein, please contact NMM (niallmm@gmail.com).

Method details

Model

The reaction-diffusion model framework used herein is substantially the same as that described in Jakobson, *et al.*, PLoS Computational Biology, 2017, in which we explored the native function of the Pdu MCP system in *S. enterica*. The analytical and numerical approach is described in detail in that manuscript, but the important assumptions can be summarized as follows:

1. We assume a spherically symmetrical organelle or scaffold at the center of a spherically symmetrical cell.
2. We consider the system at steady-state.
3. We assume that the external concentrations of the substrate (S_{ext}) and intermediate are constant.
4. We assume that the activity of the enzymes can be described by irreversible Michaelis-Menten kinetics.

The governing equations are as follows in the cytosol and in the organelle or scaffold-like structure:

Cytosol:

$$D\nabla^2 S_1(r) = 0$$

$$D\nabla^2 S_2(r) = 0$$

Organelle/scaffold:

$$D\nabla^2 S_1(r) - R_1 = 0$$

$$D\nabla^2 S_2(r) + R_1 - R_2 = 0$$

where

$$R_1 = \frac{V_1 S_1(r)}{K_1 + S_1(r)}$$

and

$$R_2 = \frac{V_2 S_2(r)}{K_2 + S_2(r)}$$

In the case of organelle- or scaffold-based organization, a closed-form analytical solution to the governing equations can be found, provided we assume that the metabolite concentration inside the organelle or scaffold region is constant. This solution is used to generate the various figures comparing organization strategies; see Jakobson et al., 2017 for the derivation and complete analytical solutions. A scaffold-like behavior is created by setting the permeability at the organelle boundary to approximate free diffusion (that is, $k_c^{S1} = k_c^{S2} \sim 10^3$). In the case with no organization, we instead use a numerical solution, as the analytical solution does not hold in this regime. The numerical solution at steady state is generated by a finite difference routine implemented in MATLAB; again see Jakobson et al., 2017 for more details on the governing equations and boundary conditions used in the numerical routine.

471 Model parameters

472 The following table summarizes the important model parameters for the Pdu MCP

473 system:

Parameter	Meaning	Estimated Value	Units
k_c^{S1}	Permeability of the Pdu MCP to propionaldehyde	10^{-5}	cm/s
k_c^{S2}	Permeability of the Pdu MCP to 1,2-PD	10^{-5}	cm/s
R_b	Radius of the bacterial cell	$5x10^{-5}$	cm
R_c	Radius of the Pdu MCP	10^{-5} (Havemann and Bobik, 2003)	cm
D	Diffusivity of metabolites in the cellular milieu	10^{-5} (Mastro et al., 1984)	cm^2/s
k_m^{S1}	Permeability of the cell membrane to propionaldehyde	10^{-2} (Robertson, 1983)	cm/s
k_m^{S2}	Permeability of the cell membrane to 1,2-PD	10^{-2} (Robertson, 1983)	cm/s
k_{catCDE}	Maximum reaction rate of a PduCDE active site	$3x10^2$ (Bachovchin et al., 1977)	1/s
N_{CDE}	Number of PduCDE enzymes per cell	$1.5x10^3$ (Havemann and Bobik, 2003)	Per cell
K_{MCDE}	Michaelis-Menten constant of PduCDE	$5x10^2$ (Bachovchin et al., 1977)	μM
k_{catPQ}	Maximum reaction rate of a PduP/Q active site	55 (Cheng and Bobik, 2012)	1/s
K_{MPQ}	Michaelis-Menten constant of PduP/Q	$1.5x10^4$ (Cheng and Bobik, 2012)	μM
N_{PQ}	Number of PduP/Q enzymes per cell	$2.5x10^3$ (Havemann and Bobik, 2003)	Per cell
S_{ext}	External 1,2-PD concentration	$5.5x10^4$ (Sampson and Bobik, 2008)	μM
A_{out}	External propionaldehyde concentration	0 (Sampson and Bobik, 2008)	μM

474

475

476 In the case of mevalonate synthesis, the parameters are altered as follows:

Parameter	Meaning	Estimated Value	Units
k_m^{S1}	Permeability of the cell membrane to acetoacetyl-CoA	10^{-4}	cm/s
k_m^{S2}	Permeability of the cell membrane to HMG-CoA	10^{-4}	cm/s
k_{catCDE}	Maximum reaction rate of a HMGS active site	1.83 (Middleton, 1972)	1/s
N_{CDE}	Number of HMGS enzymes per cell	$5x10^5$ (Dueber et al., 2009)	Per cell
K_{MCDE}	Michaelis-Menten constant of HMGS	5 (Cabañó et al., 1997)	μM
k_{catPQ}	Maximum reaction rate of a HMGR active site	0.023 (Pak et al., 2008)	1/s
K_{MPQ}	Michaelis-Menten constant of HMGR	$1x10^2$ (Pak et al., 2008)	μM
N_{PQ}	Number of HMGR enzymes per cell	$5x10^5$ (Dueber et al., 2009)	Per cell

477

478 Converting literature observations to flux predictions

479 For the systems we examine here, previous literature has described either cellular growth
480 on 1,2-PD as the sole carbon source (Sampson and Bobik, 2008) or the volumetric titer of
481 mevalonate in a scaffolded system (Dueber et al., 2009). To compare with our model,
482 which generates predictions on a molecules-per-cell basis, we must convert these
483 experimental observations to a comparable measurement.

484

485 For the native Pdu microcompartments, Sampson and Bobik observe a doubling time of
486 approximately 5-10 hours during exponential phase growth on 1,2-PD as the sole carbon
487 source (see Figure 3 of (Sampson and Bobik, 2008)). Assuming that a bacterial cell has a
488 mass of approximately 0.3 pg and that half of the flux through the microcompartment
489 pathway (by mass) can be used for cell growth, the Sampson growth observation predicts
490 a steady-state flux of approximately 3×10^{-13} μmol/cell-s.

491

492 In the case of mevalonate biosynthesis by a scaffolded system, Dueber and colleagues
493 report a titer of approximately 10 mM mevalonate after 2 days of culture, after which
494 time the concentration changes little (see Figure 5 of (Dueber et al., 2009)). Assuming
495 constant production over this time and a cell density of 2 OD~2×10^{9} cells/mL, this titer
496 corresponds to a steady-state flux of approximately 3×10^{-14} μmol/cell-s.

497

498 *Quantification and statistical analysis*

499 MATLAB R2016b (MathWorks) was used for all computation and to generate graphical
500 representations of the results.

501

502 *Data and software availability*

503 The model used herein is freely available on GitHub (URL TBD) under a GNU General
504 Public License.

505

506 **Acknowledgments**

507 This work was supported by the National Institutes of Health (grant number
508 1F32GM125162-01 to CMJ) and the National Science Foundation (award MCB1150567
509 to DTE). We thank the Tullman-Ercek and Jarosz laboratories for stimulating
510 discussions.

511 The authors declare that they have no conflict of interest.

512

513 **Author contributions**

514 CMJ, DTE, and NMM conceived of the project, analyzed results, and reviewed and
515 edited the manuscript.

516 CMJ and NMM implemented the mathematical model and wrote the original draft of the
517 manuscript.

518 DTE and NMM supervised the project.

519 **References**

520 Agapakis, C.M., Boyle, P.M., and Silver, P.A. (2012). Natural strategies for the spatial
521 optimization of metabolism in synthetic biology. Nat. Chem. Biol. *8*, 527–535.

522 Alper, H., Jin, Y.-S., Moxley, J.F., and Stephanopoulos, G. (2005). Identifying gene
523 targets for the metabolic engineering of lycopene biosynthesis in Escherichia coli.
524 Metab. Eng. *7*, 155–164.

525 Antonovsky, N., Gleizer, S., Noor, E., Zohar, Y., Herz, E., Barenholz, U., Zelcbuch, L.,
526 Amram, S., Wides, A., Tepper, N., et al. (2016). Sugar Synthesis from CO2 in
527 Escherichia coli. Cell *166*, 115–125.

528 Bachovchin, W.W., Eagar, R.G., Moore, K.W., and Richards, J.H. (1977). Mechanism of
529 action of adenosylcobalamin: glycerol and other substrate analogs as substrates and
530 inactivators for propanediol dehydratase - kinetics, stereospecificity, and
531 mechanism. Biochemistry (Mosc.) *16*, 1082–1092.

532 Beal, J., Wagner, T.E., Kitada, T., Azizgolshani, O., Parker, J.M., Densmore, D., and
533 Weiss, R. (2014). Model-Driven Engineering of Gene Expression from RNA
534 Replicons. ACS Synth. Biol. *4*, 48–56.

535 Blazeck, J., Garg, R., Reed, B., and Alper, H.S. (2012b). Controlling promoter strength
536 and regulation in Saccharomyces cerevisiae using synthetic hybrid promoters.
537 Biotechnol. Bioeng. *109*, 2884–2895.

538 Blazeck, J., Reed, B., Garg, R., Gerstner, R., Pan, A., Agarwala, V., and Alper, H.S.
539 (2012a). Generalizing a hybrid synthetic promoter approach in Yarrowia lipolytica.
540 Appl. Microbiol. Biotechnol. *97*, 3037–3052.

541 Bobik, T.A., Havemann, G.D., Busch, R.J., Williams, D.S., and Aldrich, H.C. (1999). The
542 Propanediol Utilization (pdu) Operon ofSalmonella enterica Serovar Typhimurium
543 LT2 Includes Genes Necessary for Formation of Polyhedral Organelles Involved in
544 Coenzyme B12-Dependent 1, 2-Propanediol Degradation. J. Bacteriol. *181*, 5967–
545 5975.

546 Bonacci, W., Teng, P.K., Afonso, B., Niederholtmeyer, H., Grob, P., Silver, P.A., and
547 Savage, D.F. (2012). Modularity of a carbon-fixing protein organelle. Proc. Natl. Acad.
548 Sci. *109*, 478–483.

549 Boyle, P.M., and Silver, P.A. (2012). Parts plus pipes: Synthetic biology approaches to
550 metabolic engineering. Metab. Eng. *14*, 223–232.

551 Brophy, J.A., and Voigt, C.A. (2016). Antisense transcription as a tool to tune gene
552 expression. Mol. Syst. Biol. *12*, 854.

553 Burgard, A.P., Pharkya, P., and Maranas, C.D. (2003). Optknock: A bilevel
554 programming framework for identifying gene knockout strategies for microbial
555 strain optimization. Biotechnol. Bioeng. *84*, 647–657.

556 Cabañó, J., Buesa, C., Hegardt, F.G., and Marrero, P.F. (1997). Catalytic properties of
557 recombinant 3-Hydroxy-3-Methylglutaryl Coenzyme A Synthase-1 from Blattella
558 Germanica. Insect Biochem. Mol. Biol. *27*, 499–505.

559 Cai, F., Sutter, M., Bernstein, S.L., Kinney, J.N., and Kerfeld, C.A. (2015). Engineering
560 Bacterial Microcompartment Shells: Chimeric Shell Proteins and Chimeric
561 Carboxysome Shells. ACS Synth. Biol. *4*, 444–453.

562 Cai, F., Bernstein, S.L., Wilson, S.C., and Kerfeld, C.A. (2016). Production and
563 Characterization of Synthetic Carboxysome Shells with Incorporated Luminal
564 Proteins. Plant Physiol. pp.01822.2015.

565 Chappell, J., Takahashi, M.K., and Lucks, J.B. (2015). Creating small transcription
566 activating RNAs. Nat. Chem. Biol. *11*, 214–220.

567 Chen, A.H., Robinson-Mosher, A., Savage, D.F., Silver, P.A., and Polka, J.K. (2013). The
568 Bacterial Carbon-Fixing Organelle Is Formed by Shell Envelopment of Preassembled
569 Cargo. PLoS ONE *8*, e76127.

570 Cheng, S., and Bobik, T.A. (2012). The PduQ Enzyme Is an Alcohol Dehydrogenase
571 Used to Recycle NAD+ Internally within the Pdu Microcompartment of Salmonella
572 enterica.

573 Conrado, R.J., Wu, G.C., Boock, J.T., Xu, H., Chen, S.Y., Lebar, T., Turnsek, J., Tomsic, N.,
574 Avbelj, M., Gaber, R., et al. (2012). DNA-guided assembly of biosynthetic pathways
575 promotes improved catalytic efficiency. Nucleic Acids Res. *40*, 1879–1889.

576 Dahl, R.H., Zhang, F., Alonso-Gutierrez, J., Baidoo, E., Batth, T.S., Redding-Johanson,
577 A.M., Petzold, C.J., Mukhopadhyay, A., Lee, T.S., Adams, P.D., et al. (2013).
578 Engineering dynamic pathway regulation using stress-response promoters. Nat.
579 Biotechnol. *31*, 1039–1046.

580 Delebecque, C.J., Lindner, A.B., Silver, P.A., and Aldaye, F.A. (2011). Organization of
581 Intracellular Reactions with Rationally Designed RNA Assemblies. Science *333*, 470–
582 474.

583 Ducat, D.C., and Silver, P.A. (2012). Improving Carbon Fixation Pathways. Curr. Opin.
584 Chem. Biol. *16*, 337–344.

585 Dudley, Q.M., Anderson, K.C., and Jewett, M.C. (2016). Cell-Free Mixing of Escherichia
586 coli Crude Extracts to Prototype and Rationally Engineer High-Titer Mevalonate
587 Synthesis. ACS Synth. Biol.

588 Dueber, J.E., Wu, G.C., Malmirchegini, G.R., Moon, T.S., Petzold, C.J., Ullal, A.V., Prather,
589 K.L., and Keasling, J.D. (2009). Synthetic protein scaffolds provide modular control
590 over metabolic flux. Nat. Biotechnol. *27*, 753–759.

591 Fan, C., Cheng, S., Liu, Y., Escobar, C.M., Crowley, C.S., Jefferson, R.E., Yeates, T.O., and
592 Bobik, T.A. (2010). Short N-terminal sequences package proteins into bacterial
593 microcompartments. Proc. Natl. Acad. Sci. *107*, 7509–7514.

594 Fernandez-Rodriguez, J., and Voigt, C.A. (2016). Post-translational control of genetic
595 circuits using Potyvirus proteases. Nucleic Acids Res. *44*, 6493–6502.

596 Garamella, J., Marshall, R., Rustad, M., and Noireaux, V. (2016). The All E. coli TX-TL
597 Toolbox 2.0: A Platform for Cell-Free Synthetic Biology. ACS Synth. Biol. *5*, 344–355.

598 Giessen, T.W., and Silver, P.A. (2017). Engineering carbon fixation with artificial
599 protein organelles. Curr. Opin. Biotechnol. *46*, 42–50.

600 Goering, A.W., Li, J., McClure, R.A., Thomson, R.J., Jewett, M.C., and Kelleher, N.L.
601 (2016). In Vitro Reconstruction of Nonribosomal Peptide Biosynthesis Directly from
602 DNA Using Cell-Free Protein Synthesis. ACS Synth. Biol.

603 Gonzalez-Esquer, C.R., Shubitowski, T.B., and Kerfeld, C.A. (2015). Streamlined
604 Construction of the Cyanobacterial CO2-Fixing Organelle via Protein Domain
605 Fusions for Use in Plant Synthetic Biology. Plant Cell tpc.15.00329.

606 Goodman, D.B., Church, G.M., and Kosuri, S. (2013). Causes and Effects of N-Terminal
607 Codon Bias in Bacterial Genes. Science.

608 Hanson, M.R., Lin, M.T., Carmo-Silva, A.E., and Parry, M.A.J. (2016). Towards
609 engineering carboxysomes into C3 plants. Plant J. *87*, 38–50.

610 Havemann, G.D., and Bobik, T.A. (2003). Protein content of polyhedral organelles
611 involved in coenzyme B12-dependent degradation of 1, 2-propanediol in Salmonella
612 enterica serovar Typhimurium LT2. J. Bacteriol. *185*, 5086–5095.

613 Hinzpeter, F., Gerland, U., and Tostevin, F. (2017). Optimal Compartmentalization
614 Strategies for Metabolic Microcompartments. Biophys. J. *112*, 767–779.

615 Huseby, D.L., and Roth, J.R. (2013). Evidence that a Metabolic Microcompartment
616 Contains and Recycles Private Cofactor Pools. J. Bacteriol. *195*, 2864–2879.

617 Jakobson, C.M., Kim, E.Y., Slininger, M.F., Chien, A., and Tullman-Ercek, D. (2015).
618 Localization of Proteins to the 1,2-Propanediol Utilization Microcompartment by
619 Non-native Signal Sequences Is Mediated by a Common Hydrophobic Motif. J. Biol.
620 Chem. *290*, 24519–24533.

621 Jakobson, C.M., Chen, Y., Slininger, M.F., Valdivia, E., Kim, E.Y., and Tullman-Ercek, D.
622 (2016). Tuning the Catalytic Activity of Subcellular Nanoreactors. J. Mol. Biol.

623 Jakobson, C.M., Tullman-Ercek, D., Slininger, M.F., and Mangan, N.M. (2017). A
624 systems-level model reveals that 1,2-Propanediol utilization microcompartments
625 enhance pathway flux through intermediate sequestration. PLOS Comput. Biol. *13*,
626 e1005525.

627 Kelly, T.J., and Smith, H.O. (1970). A restriction enzyme from Hemophilus influenzae.
628 J. Mol. Biol. *51*, 393–409.

629 Kerfeld, C.A. (2017). A bioarchitectonic approach to the modular engineering of
630 metabolism. Phil Trans R Soc B *372*, 20160387.

631 Kerfeld, C.A., Sawaya, M.R., Tanaka, S., Nguyen, C.V., Phillips, M., Beeby, M., and
632 Yeates, T.O. (2005). Protein structures forming the shell of primitive bacterial
633 organelles. Science *309*, 936–938.

634 Khosla, C., Herschlag, D., Cane, D.E., and Walsh, C.T. (2014). Assembly Line
635 Polyketide Synthases: Mechanistic Insights and Unsolved Problems. Biochemistry
636 (Mosc.) *53*, 2875–2883.

637 Kim, E.Y., and Tullman-Ercek, D. (2013). Engineering nanoscale protein
638 compartments for synthetic organelles. Curr. Opin. Biotechnol. *24*, 627–632.

639 Kim, E.Y., Jakobson, C.M., and Tullman-Ercek, D. (2014). Engineering Transcriptional
640 Regulation to Control Pdu Microcompartment Formation. PLoS ONE *9*, e113814.

641 Kim, H.U., Kim, T.Y., and Lee, S.Y. (2008). Metabolic flux analysis and metabolic
642 engineering of microorganisms. Mol. BioSyst. *4*, 113–120.

643 Kofoid, E., Rappleye, C., Stojiljkovic, I., and Roth, J. (1999). The 17-Gene
644 Ethanolamine (eut) Operon ofSalmonella typhimurium Encodes Five Homologues of
645 Carboxysome Shell Proteins. J. Bacteriol. *181*, 5317–5329.

646 Lawrence, A.D., Frank, S., Newnham, S., Lee, M.J., Brown, I.R., Xue, W.-F., Rowe, M.L.,
647 Mulvihill, D.P., Prentice, M.B., Howard, M.J., et al. (2014). Solution Structure of a
648 Bacterial Microcompartment Targeting Peptide and Its Application in the
649 Construction of an Ethanol Bioreactor. ACS Synth. Biol. 140224092559007.

650 Leavitt, J.M., Tong, A., Tong, J., Pattie, J., and Alper, H.S. (2016). Coordinated
651 transcription factor and promoter engineering to establish strong expression
652 elements in Saccharomyces cerevisiae. Biotechnol. J. *11*, 866–876.

653 Lechner, A., Brunk, E., and Keasling, J.D. (2016). The Need for Integrated Approaches
654 in Metabolic Engineering. Cold Spring Harb. Perspect. Biol. *8*, a023903.

655 Lee, M.E., Aswani, A., Han, A.S., Tomlin, C.J., and Dueber, J.E. (2013). Expression-level
656 optimization of a multi-enzyme pathway in the absence of a high-throughput assay.
657 Nucleic Acids Res. *41*, 10668–10678.

658 Lee, M.E., DeLoache, W.C., Cervantes, B., and Dueber, J.E. (2015). A Highly
659 Characterized Yeast Toolkit for Modular, Multipart Assembly. ACS Synth. Biol. *4*,
660 975–986.

661 Lin, M.T., Occhialini, A., Andralojc, P.J., Parry, M.A.J., and Hanson, M.R. (2014a). A
662 faster Rubisco with potential to increase photosynthesis in crops. Nature *513*, 547–
663 550.

664 Lin, M.T., Occhialini, A., Andralojc, P.J., Devonshire, J., Hines, K.M., Parry, M.A.J., and
665 Hanson, M.R. (2014b). β-Carboxysomal proteins assemble into highly organized
666 structures in Nicotiana chloroplasts. Plant J. Cell Mol. Biol. *79*, 1–12.

667 Long, B.M., Rae, B.D., Rolland, V., Förster, B., and Price, G.D. (2016). Cyanobacterial
668 CO2-concentrating mechanism components: function and prospects for plant
669 metabolic engineering. Curr. Opin. Plant Biol. *31*, 1–8.

670 Long, S.P., Marshall-Colon, A., and Zhu, X.-G. (2015). Meeting the Global Food
671 Demand of the Future by Engineering Crop Photosynthesis and Yield Potential. Cell
672 *161*, 56–66.

673 Lopez, G., and Anderson, J.C. (2015). Synthetic Auxotrophs with Ligand-Dependent
674 Essential Genes for a BL21(DE3) Biosafety Strain. ACS Synth. Biol. *4*, 1279–1286.

675 Lu, F., Smith, P.R., Mehta, K., and Swartz, J.R. (2015). Development of a synthetic
676 pathway to convert glucose to hydrogen using cell free extracts. Int. J. Hydrog.
677 Energy *40*, 9113–9124.

678 Lu, Y., Welsh, J.P., and Swartz, J.R. (2014). Production and stabilization of the
679 trimeric influenza hemagglutinin stem domain for potentially broadly protective
680 influenza vaccines. Proc. Natl. Acad. Sci. *111*, 125–130.

681 Mandell, D.J., Lajoie, M.J., Mee, M.T., Takeuchi, R., Kuznetsov, G., Norville, J.E., Gregg,
682 C.J., Stoddard, B.L., and Church, G.M. (2015). Biocontainment of genetically modified
683 organisms by synthetic protein design. Nature *518*, 55–60.

684 Mangan, N.M., and Brenner, M.P. (2014). Systems analysis of the CO2 concentrating
685 mechanism in cyanobacteria. eLife *3*, e02043.

686 Mangan, N.M., Flamholz, A., Hood, R.D., Milo, R., and Savage, D.F. (2016). pH
687 determines the energetic efficiency of the cyanobacterial CO2 concentrating
688 mechanism. Proc. Natl. Acad. Sci. *113*, E5354–E5362.

689 Marchand, N., and Collins, C.H. (2016). Synthetic Quorum Sensing and Cell–Cell
690 Communication in Gram-Positive Bacillus megaterium. ACS Synth. Biol. *5*, 597–606.

691 Mastro, A.M., Babich, M.A., Taylor, W.D., and Keith, A.D. (1984). Diffusion of a small
692 molecule in the cytoplasm of mammalian cells. Proc. Natl. Acad. Sci. *81*, 3414–3418.

693 McHugh, C.A., Fontana, J., Nemecek, D., Cheng, N., Aksyuk, A.A., Heymann, J.B.,
694 Winkler, D.C., Lam, A.S., Wall, J.S., Steven, A.C., et al. (2014). A virus capsid-like
695 nanocompartment that stores iron and protects bacteria from oxidative stress.
696 EMBO J. *33*, 1896–1911.

697 Middleton, B. (1972). The kinetic mechanism of 3-hydroxy-3-methylglutaryl-
698 coenzyme A synthase from baker's yeast. Biochem. J. *126*, 35–47.

699 Moon, T.S., Dueber, J.E., Shiue, E., and Prather, K.L.J. (2010). Use of modular,
700 synthetic scaffolds for improved production of glucaric acid in engineered E. coli.
701 Metab. Eng. *12*, 298–305.

702 Mukherjee, K., Bhattacharyya, S., and Peralta-Yahya, P. (2015). GPCR-Based
703 Chemical Biosensors for Medium-Chain Fatty Acids. ACS Synth. Biol. *4*, 1261–1269.

704 Mutalik, V.K., Guimaraes, J.C., Cambray, G., Lam, C., Christoffersen, M.J., Mai, Q.-A.,
705 Tran, A.B., Paull, M., Keasling, J.D., Arkin, A.P., et al. (2013). Precise and reliable gene
706 expression via standard transcription and translation initiation elements. Nat.
707 Methods *10*, 354–360.

708 Myhrvold, C., Polka, J.K., and Silver, P.A. (2016). Synthetic Lipid-Containing Scaffolds
709 Enhance Production by Colocalizing Enzymes. ACS Synth. Biol. *5*, 1396–1403.

710 Nielsen, A.A.K., Der, B.S., Shin, J., Vaidyanathan, P., Paralanov, V., Strychalski, E.A.,
711 Ross, D., Densmore, D., and Voigt, C.A. (2016). Genetic circuit design automation.
712 Science *352*, aac7341.

713 Noor, E., Flamholz, A., Bar-Even, A., Davidi, D., Milo, R., and Liebermeister, W. (2016).
714 The Protein Cost of Metabolic Fluxes: Prediction from Enzymatic Rate Laws and Cost
715 Minimization. PLOS Comput. Biol. *12*, e1005167.

716 Paddon, C.J., Westfall, P.J., Pitera, D.J., Benjamin, K., Fisher, K., McPhee, D., Leavell,
717 M.D., Tai, A., Main, A., Eng, D., et al. (2013). High-level semi-synthetic production of
718 the potent antimalarial artemisinin. Nature *496*, 528–532.

719 Pak, V.V., Koo, M., Kim, M.J., Yang, H.J., Yun, L., and Kwon, D.Y. (2008). Modeling an
720 active conformation for linear peptides and design of a competitive inhibitor for
721 HMG-CoA reductase. J. Mol. Recognit. JMR *21*, 224–232.

722 Park, J., Chun, S., Bobik, T.A., Houk, K.N., and Yeates, T.O. (2017). Molecular Dynamics
723 Simulations of Selective Metabolite Transport across the Propanediol Bacterial
724 Microcompartment Shell. J. Phys. Chem. B.

725 Parsons, J.B., Frank, S., Bhella, D., Liang, M., Prentice, M.B., Mulvihill, D.P., and
726 Warren, M.J. (2010). Synthesis of Empty Bacterial Microcompartments, Directed
727 Organelle Protein Incorporation, and Evidence of Filament-Associated Organelle
728 Movement. Mol. Cell *38*, 305–315.

729 Peng, X. "Nick," Gilmore, S.P., and O'Malley, M.A. (2016). Microbial communities for
730 bioprocessing: lessons learned from nature. Curr. Opin. Chem. Eng. *14*, 103–109.

731 Polka, J.K., Hays, S.G., and Silver, P.A. (2016). Building Spatial Synthetic Biology with
732 Compartments, Scaffolds, and Communities. Cold Spring Harb. Perspect. Biol. *8*.

733 Price, N.D., Reed, J.L., and Palsson, B.Ø. (2004). Genome-scale models of microbial
734 cells: evaluating the consequences of constraints. Nat. Rev. Microbiol. *2*, 886–897.

735 Purcell, O., and Lu, T.K. (2014). Synthetic analog and digital circuits for cellular
736 computation and memory. Curr. Opin. Biotechnol. *29*, 146–155.

737 Rae, B.D., Long, B.M., Förster, B., Nguyen, N.D., Velanis, C.N., Atkinson, N., Hee, W.Y.,
738 Mukherjee, B., Price, G.D., and McCormick, A.J. (2017). Progress and challenges of
739 engineering a biophysical carbon dioxide-concentrating mechanism into higher
740 plants. J. Exp. Bot.

741 Rajkumar, A.S., Liu, G., Bergenholm, D., Arsovska, D., Kristensen, M., Nielsen, J.,
742 Jensen, M.K., and Keasling, J.D. (2016). Engineering of synthetic, stress-responsive
743 yeast promoters. Nucleic Acids Res. gkw553.

744 Ranganathan, S., Suthers, P.F., and Maranas, C.D. (2010). OptForce: An Optimization
745 Procedure for Identifying All Genetic Manipulations Leading to Targeted
746 Overproductions. PLOS Comput Biol *6*, e1000744.

747 Robertson, R.N. (1983). Lively Membranes (CUP Archive).

748 Roehner, N., Young, E.M., Voigt, C.A., Gordon, D.B., and Densmore, D. (2016). Double
749 Dutch: A Tool for Designing Combinatorial Libraries of Biological Systems. ACS
750 Synth. Biol. *5*, 507–517.

751 Salis, H.M., Mirsky, E.A., and Voigt, C.A. (2009). Automated design of synthetic
752 ribosome binding sites to control protein expression. Nat. Biotechnol. *27*, 946–950.

753 Sampson, E.M., and Bobik, T.A. (2008). Microcompartments for B12-Dependent 1,2-
754 Propanediol Degradation Provide Protection from DNA and Cellular Damage by a
755 Reactive Metabolic Intermediate. J. Bacteriol. *190*, 2966–2971.

Sharwood, R.E., Ghannoum, O., and Whitney, S.M. (2016). Prospects for improving CO2 fixation in C3-crops through understanding C4-Rubisco biogenesis and catalytic diversity. Curr. Opin. Plant Biol. *31*, 135–142.

Shively, J., Ball, F., and Kline, B. (1973). Electron Microscopy of the Carboxysomes (Polyhedral Bodies) of Thiobacillus neapolitanus. J. Bacteriol. *116*, 1405–1411.

Slininger Lee, M.F., Jakobson, C.M., and Tullman-Ercek, D. (2017). Evidence for Improved Encapsulated Pathway Behavior in a Bacterial Microcompartment through Shell Protein Engineering. ACS Synth. Biol.

Smith, H.O., and Welcox, K.W. (1970). A Restriction enzyme from Hemophilus influenzae. J. Mol. Biol. *51*, 379–391.

Srivastava, S., Kotker, J., Hamilton, S., Ruan, P., Tsui, J., Anderson, J.C., Bodik, R., and Seshia, S. (2012). Pathway Synthesis using the Act Ontology. 4th Int. Workshop Bio-Des. Autom. IWBDA.

Sullivan, C.J., Pendleton, E.D., Sasmor, H.H., Hicks, W.L., Farnum, J.B., Muto, M., Amendt, E.M., Schoborg, J.A., Martin, R.W., Clark, L.G., et al. (2016). A cell-free expression and purification process for rapid production of protein biologics. Biotechnol. J. *11*, 238–248.

Takahashi, M.K., and Lucks, J.B. (2013). A modular strategy for engineering orthogonal chimeric RNA transcription regulators. Nucleic Acids Res. *41*, 7577–7588.

Wagner, H.J., Capitain, C.C., Richter, K., Nessling, M., and Mampel, J. (2016). Engineering bacterial microcompartments with heterologous enzyme cargos. Eng. Life Sci. n/a-n/a.

Walker, M.C., Thuronyi, B.W., Charkoudian, L.K., Lowry, B., Khosla, C., and Chang, M.C.Y. (2013). Expanding the Fluorine Chemistry of Living Systems Using Engineered Polyketide Synthase Pathways. Science *341*, 1089–1094.

Worst, E.G., Exner, M.P., De Simone, A., Schenkelberger, M., Noireaux, V., Budisa, N., and Ott, A. (2015). Cell-free expression with the toxic amino acid canavanine. Bioorg. Med. Chem. Lett. *25*, 3658–3660.

Wu, F., and Minteer, S. (2014). Krebs Cycle Metabolon: Structural Evidence of Substrate Channeling Revealed by Cross-Linking and Mass Spectrometry. Angew. Chem. Int. Ed. n/a-n/a.

Xu, P., Li, L., Zhang, F., Stephanopoulos, G., and Koffas, M. (2014). Improving fatty acids production by engineering dynamic pathway regulation and metabolic control. Proc. Natl. Acad. Sci. *111*, 11299–11304.

791 Yang, L., Dolan, E.M., Tan, S.K., Lin, T., Sontag, E.D., and Khare, S. (2017).
792 Computation-guided design of a stimulus-responsive multi-enzyme supramolecular
793 assembly. ChemBioChem n/a-n/a.

794 Zhang, Y., Tsitkov, S., and Hess, H. (2016). Proximity does not contribute to activity
795 enhancement in the glucose oxidase–horseradish peroxidase cascade. Nat. Commun.
796 *7*, 13982.

797 Zhu, X., Liu, J., and Zhang, W. (2015). De novo biosynthesis of terminal alkyne-
798 labeled natural products. Nat. Chem. Biol. *11*, 115–120.

799

800 **Figure Legends**

801 **Figure 1.** (A) Roadblocks commonly facing heterologous biosynthesis. (B) Potential
802 organization strategies to alleviate these roadblocks. (C) Schematics of our models of
803 (left) a pathway without organization, (middle) a pathway organized on a scaffold, and
804 (right) a pathway organized in an organelle.

805

806 **Figure 2.** Relevant substrates, intermediates, products, and enzyme kinetic parameters for
807 (A) native Pdu microcompartment metabolism and (B) mevalonate biosynthesis.
808 Predicted pathway flux for (C) native Pdu microcompartment metabolism and (D)
809 mevalonate biosynthesis for native kinetics without organization; 100-fold improvement
810 of k_{cat} for both pathway enzymes; 100-fold improvement in K_M for both pathway
811 enzymes; native kinetics with organization on a scaffold; and native kinetics with
812 organization in a microcompartment organelle. The predictions here are based on an
813 external substrate concentration of 50 mM 1,2-propanediol, as is typically used in
814 experiments (Sampson and Bobik, 2008). We use the same external substrate
815 concentration (50 mM) in the mevalonate case. Experimental observations in (C) and (D)
816 are calculated from *S. enterica* growth rates from Sampson and Bobik, 2008 and from
817 titer measurements for a scaffolded system from Dueber et al., 2009.

818

819 **Figure 3.** (A) Predicted flux for (left) native Pdu microcompartment metabolism and
820 (right) mevalonate biosynthesis without organization (grey); with organization on a
821 scaffold (orange); and with organization in an organelle (blue) as a function of external
822 substrate concentration S_{ext}. (B) Predicted intermediate leakage for (left) native Pdu

823 microcompartment metabolism and (right) mevalonate biosynthesis without organization
824 (grey); with organization on a scaffold (orange); and with organization in an organelle
825 (blue) as a function of external substrate concentration S_{ext}. (C) Predicted optimal
826 organizational strategy for (left) native Pdu microcompartment metabolism and (right)
827 mevalonate biosynthesis as a function of external substrate concentration S_{ext} and the
828 abundance and kinetics of the second pathway enzyme $k_{cat}E_0$ (PduP/Q and HMGR,
829 respectively). Baseline parameter values are shown with a black dashed line. (D)
830 Predicted optimal organizational strategy for native Pdu microcompartment metabolism
831 (magenta) and mevalonate biosynthesis (purple) as a function of the abundance and
832 kinetics of the second pathway enzyme $k_{cat}E_0$ (PduP/Q and HMGR, respectively) and the
833 cell membrane permeability to the intermediate at (left) external substrate concentration
834 S_{ext} = 50 mM and (right) S_{ext} = 0.5 mM. Regions of parameter space are colored by the
835 optimal organization strategy in that region: organelle (blue); scaffold (orange); or no
836 organization (grey).
837
838 **Figure 4.** Recommended organization strategy resulting in (left) maximum pathway flux
839 or (right) minimum intermediate leakage for native Pdu metabolism as a function of (A)
840 $k_{cat}E_0$ of PduCDE and PduP/Q, (B) organelle permeability and K_M of PduP/Q, and (C)
841 organelle permeability and cell membrane permeability. Regions of parameter space are
842 colored by the optimal organization strategy in that region: organelle (blue); scaffold
843 (orange); or no organization (grey). Baseline parameter values are shown with a black
844 dashed line.

Figures

To accompany: Spatially organizing biochemistry: choosing a strategy to translate synthetic biology to the factory

Christopher M. Jakobson, Danielle Tullman-Ercek, Niall M. Mangan

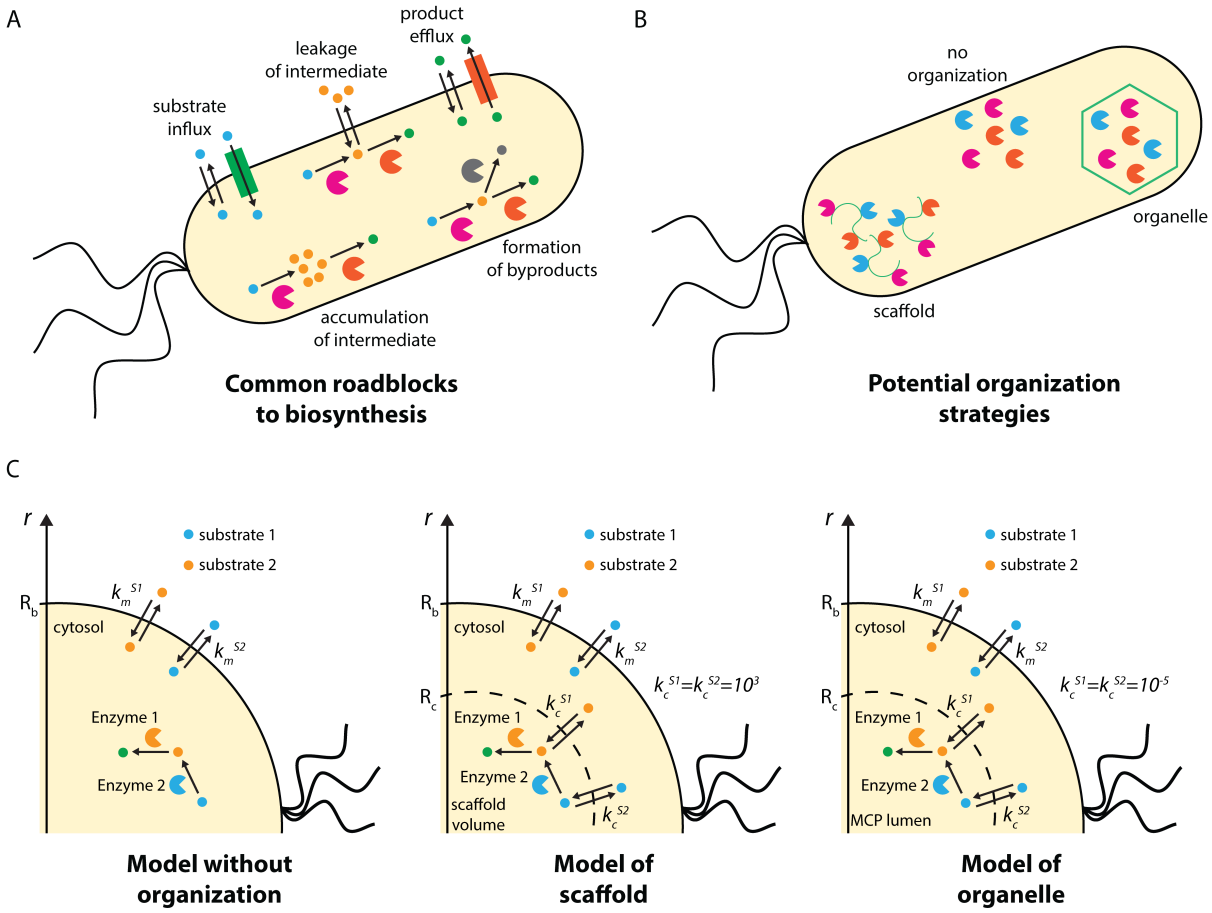

Figure 1.

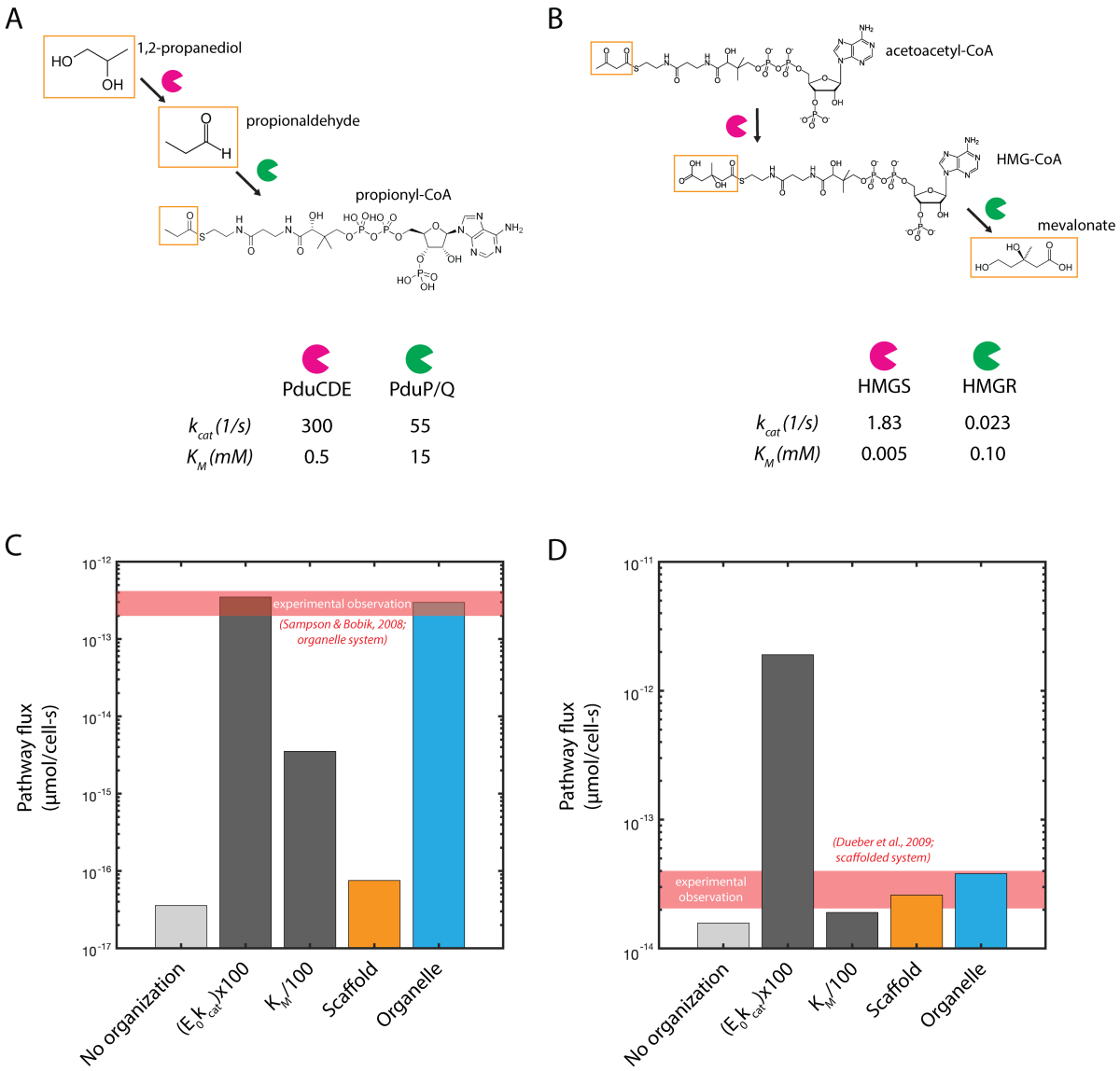

Figure 2.

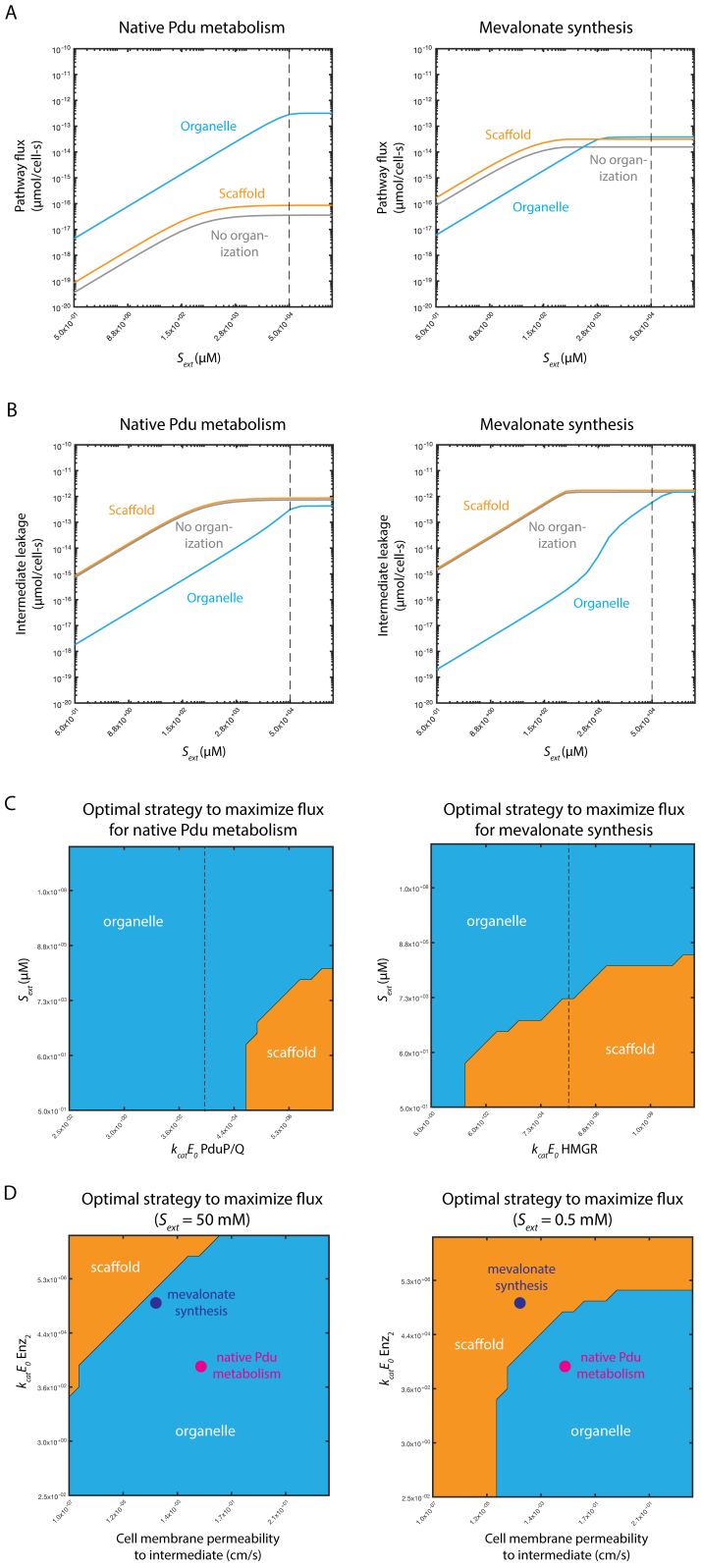

Figure 3.

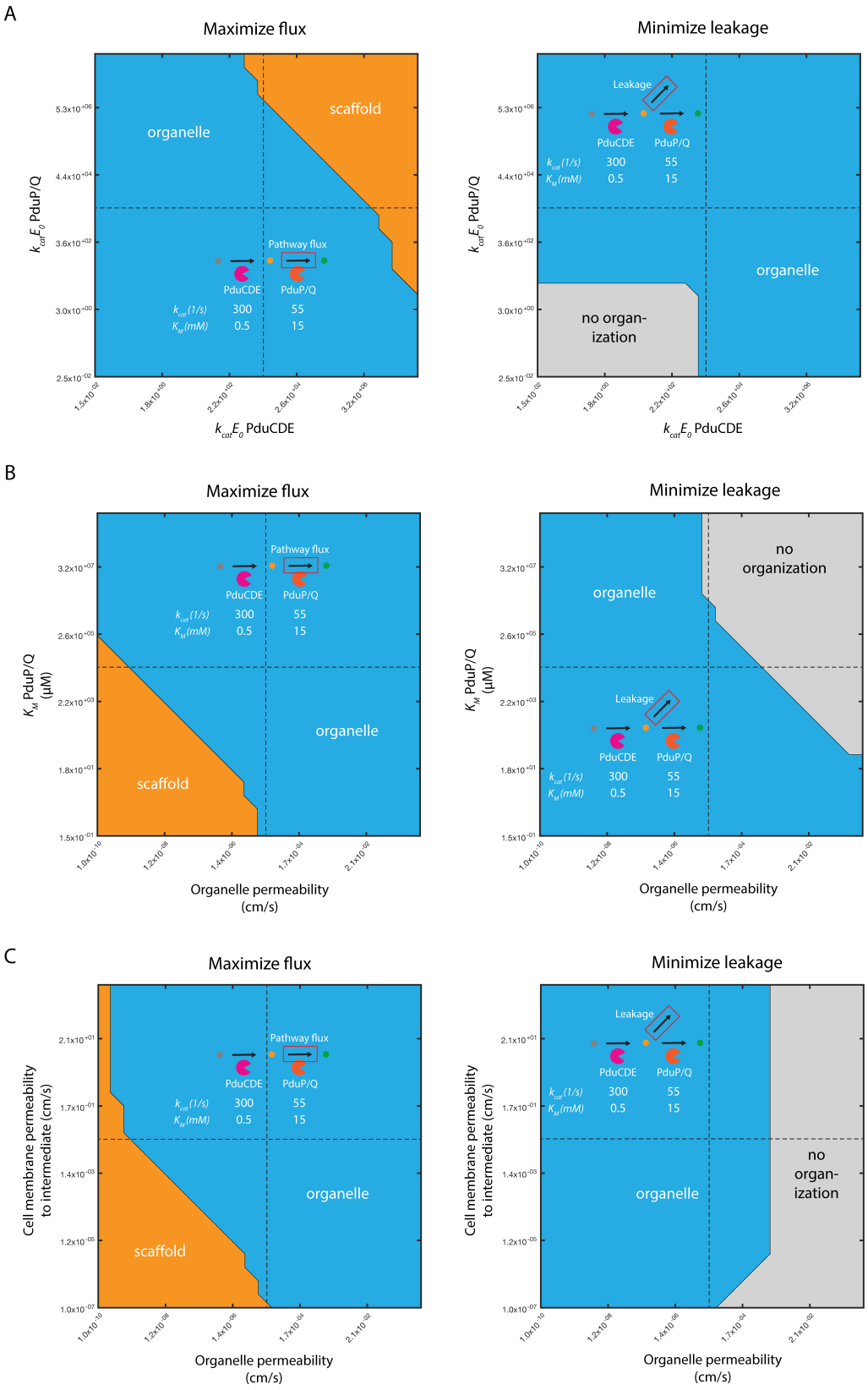

Figure 4.